Wave Run-Up on Dikes with Shallow Foreshores

Article *in* Journal of Waterway Port Coastal and Ocean Engineering · March 2001

DOI: 10.1061/(ASCE)0733-950X(2001)127:5(254)

1 author:

Marcel R.A. van Gent
Deltares
102 PUBLICATIONS **951** CITATIONS

SEE PROFILE

WAVE RUNUP ON DIKES WITH SHALLOW FORESHORES

By Marcel R. A. van Gent[1]

ABSTRACT: Prototype measurements, physical model tests, and numerical model computations have been performed and combined to study wave runup on dikes with shallow foreshores. Shallow foreshores considerably affect the evolution of wave height distributions and wave energy spectra between deep water and the toe of coastal structures. The numerical model investigations were performed to study the influence of wave energy spectra on wave runup and wave overtopping. This resulted in a characteristic wave period for wave runup and wave overtopping, which takes the effects of wave energy spectra into account. This was confirmed in a series of physical model tests with different types of foreshores and different types of structures. Also, results from physical model tests were compared with results from measurements in prototype. The six storm conditions that were measured in prototype were accurately reproduced in the physical model tests. The results of each of the three data sources were combined, and led to a prediction method that can be used for conditions with deep water and for conditions with shallow foreshores.

INTRODUCTION

Due to combinations of swell and sea or due to processes on the foreshore, wave energy spectra at the toe of coastal structures often are double or multipeaked. Shallow foreshores may also change considerably the wave height distributions compared to those in deeper water. Both may affect wave runup and wave overtopping. The approach followed here is to find one characteristic wave height and one characteristic wave period that can be used in the surf-similarity parameter (or ''Iribarren number'') to take the effects of wave height distributions and wave energy spectra, respectively, into account. In this paper, most emphasis is put on the effects of wave energy spectra on wave runup (characterized by the parameter $z_{2\%}$, which is the wave runup level exceeded by 2% of the incident waves), although the research reports on which this paper is based also cover the effects of wave height distributions and the effects on wave overtopping (van Gent 1999b,c).

In this paper, first numerical model results are analyzed to study the influence of wave energy spectra on wave runup. Then physical model investigations are described to study the same topic. A part of the described physical model tests was also performed to reproduce storms measured in prototype to gain insight into the differences between both types of measurements.

NUMERICAL MODELING

The numerical model applied here is a time-domain model that simulates wave motion on coastal structures (van Gent 1994, 1995). The model simulates perpendicular wave attack on structures using the nonlinear shallow-water wave equations. Steep wave fronts are represented by bores. Use is made of an explicit dissipative finite-difference scheme (Lax-Wendroff). Hibberd and Peregrine (1979) used this concept for impermeable slopes without roughness. Similar models have been shown to predict well wave reflection and wave runup on impermeable rough slopes (Kobayashi et al. 1987). In van Gent (1994, 1995), the extension of the model to simulate wave interaction with permeable coastal structures is described, as well as a validation of the model for wave runup and wave overtopping. In van Gent and Doorn (2001), an additional validation of the model for wave runup is discussed.

A numerical data set, where irregular waves are generated at the toe of the structure, was created with 1:2.5 and 1:4 slopes, while the water depth and the wave height at the toe of the structures were constant ($d_{\mathrm{TOE}} = 0.7$ m and $H_{m0} = 0.148$ m). The wave height distributions approximate a Rayleigh distribution. The numerical parameters were taken constant in all computations; $\Delta x = 0.05$ m and $\Delta t = 0.005$ s [at least 75 space steps per wavelength based on the peak wave period and a CFL number of $\sqrt{(g d_{\mathrm{TOE}})}\Delta t/\Delta x = 0.26$]. The friction coefficient was set at $f = 0.1$ in all computations. According to tests by Cornett and Mansard (1995), this roughly corresponds to the roughness of stones of $D_{n50} = 0.01$ m at the slope. Compared to the friction factors in wave runup formulas proposed by De Waal and van der Meer (1993), such roughness reduces the wave runup by a factor of about $\gamma_f = 0.7$ compared to a very smooth slope. This estimate of the reduction factor due to roughness is not very important for this study because the analysis is mainly based on the scatter around main trends rather than on exact values of the computed wave runup.

The numerical data set consisted of single-peaked wave energy spectra and double-peaked wave energy spectra. The double-peaked wave energy spectra were generated by superposition of two single-peaked wave energy spectra; the amounts of energy per peak and the distances between the two peaks were varied. The spectral shapes were TMA spectra (a JONSWAP spectrum adapted for finite water depth) (Bouws et al. 1985). The amount of energy and the position of the peaks of each wave energy spectrum are denoted by $m_{0(1)}$, $m_{0(2)}$ and T_{p1}, T_{p2}, respectively. The ratio of the two peak periods was varied; $T_{p2}/T_{p1} = 0.3$, 0.45, 0.6, and 0.75. For each combination, the amount of energy in each peak was varied; $m_{0(2)}/m_{0(1)} = 0.5$, 1.0, and 2.0. In total, two slope angles, six basic wave periods, four distances between the two peaks, and three different energy ratios are used, which leads to a total matrix of $2 \cdot 6 \cdot 4 \cdot 3 = 144$ double-peaked spectra plus 12 single-peaked wave energy spectra. An additional set of 39 computations has been performed for the 1:2.5 slope, where double-peaked wave energy spectra were generated by superposition of two Pierson-Moskowitz (PM) spectra instead of two TMA spectra. These PM spectra are broader than TMA spectra. Analysis of the results has been performed irrespective of the basic spectral shape (PM or TMA) used. In total, a numerical data set of 195 computations, each with 500–800 individual waves, was generated for studying wave runup.

To account for the effects of double-peaked wave energy spectra on wave runup, several methods exist. For instance,

[1]Dr., Mgr., Wave Dynamics and Structures Group, WL 1, Delft Hydraulics, P.O. Box 177, 2600 MH, Delft, The Netherlands. E-mail: marcel.vangent@wldelft.nl

Note. Discussion open until March 1, 2002. To extend the closing date one month, a written request must be filed with the ASCE Manager of Journals. The manuscript for this paper was submitted for review and possible publication on October 26, 2000; revised April 6, 2001. This paper is part of the ***Journal of Waterway, Port, Coastal, and Ocean Engineering***, Vol. 127, No. 5, September/October, 2001. ©ASCE, ISSN 0733-950X/01/0005-0254–0262/$8.00 + $.50 per page. Paper No. 22215.

J. Waterway, Port, Coastal, Ocean Eng. 2001.127:254-262.

Seijffert (1991) and van der Meer (1997) proposed geometric methods. In these geometric methods, two peaks of the wave energy spectra are detected. These two peaks play a role in either defining an alternative wave period or in defining imaginary wave runup levels for each separate peak, while weight factors are used to obtain a prediction of the real wave runup. More generic methods can be developed that do not make use of geometric approaches, but use spectral moments of the wave energy spectrum. These methods allow for predictions for more arbitrarily shaped wave energy spectra, which can be single peaked, double peaked, or multipeaked, without the need for detection of local peaks in the wave energy spectrum. In Holterman (1998), several alternative wave periods based on spectral moments were considered for use in runup formulas. Due to limited data on wave runup for double or multipeaked spectra, no clear conclusions on the optimal choice of characteristic wave period could be given. Although this subject has been studied before based on physical model tests (Van Oorschot and d'Angremond 1969), here also use is made of numerical model investigations where the wave energy spectra at the toe of the structure form the basis for analysis.

Figs. 1 and 2 show the results of the wave runup computations as a function of the surf-similarity parameters, where two different characteristic wave periods were used—the peak wave period T_p, which is based on the global maximum of the wave energy spectrum, and the spectral wave period $T_{m-1,0}$, which is based on the spectral moments m_{-1} and m_0 ($T_{m-1,0} = m_{-1}/m_0$, where $m_n = {}_0\int^{\infty} f^n S(f)\, df$). In these figures, the reduction factor for friction $\gamma = 0.7$ is used, since this was expected to correspond to the friction factor $f = 0.1$ used in the computations. Based on visual inspection of Figs. 1 and 2, the following conclusions can be drawn:

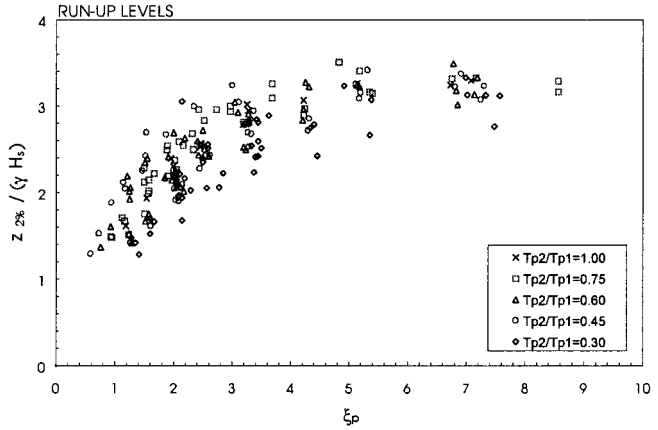

FIG. 1. Computed 2% Wave Runup Levels As Function of the Surf-Similarity Parameter Based on the Peak Wave Period T_p

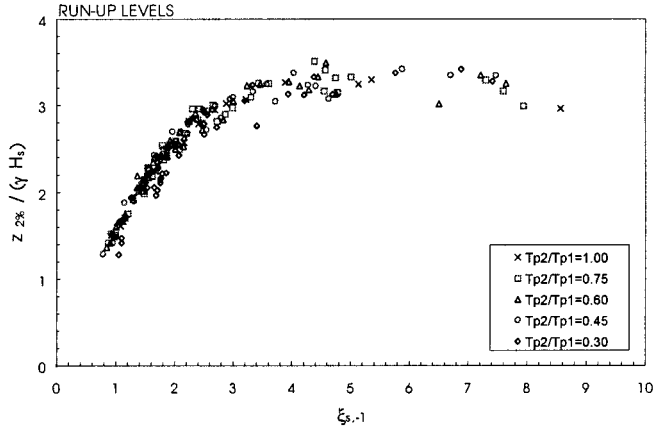

FIG. 2. Computed 2% Wave Runup Levels As Function of the Surf-Similarity Parameter Based on the Wave Period $T_{m-1,0}$

- The amount of scatter in Fig. 1 indicates that the peak wave period T_p is not an appropriate parameter to predict wave runup for situations with double-peaked wave energy spectra.
- Fig. 2 shows that if the wave period $T_{m-1,0}$ is used in the surf-similarity parameter, all data are more or less of the same trend, which indicates that if this wave period is used in the surf-similarity parameter, there is almost no influence of the distance between the two separate peaks of the double-peaked wave energy spectra.

To study which of the wave periods might be the optimal characteristic wave period, a formula [(1)] was used, which describes the main trend through the data points. This formula will be discussed in more detail later in this paper

$$z_{2\%}/(\gamma H_s) = c_0 \xi \qquad \text{for } \xi \le p \tag{1a}$$

$$z_{2\%}/(\gamma H_s) = c_1 - c_2/\xi \quad \text{for } \xi \ge p \tag{1b}$$

where H_s = significant wave height of the incident waves at the toe of the structure ($H_s = H_{1/3}$). The reduction factor γ takes the effects of roughness into account. The surf-similarity parameter is defined as $\xi = \tan\varphi/\sqrt{(2\pi/g \cdot H_s/T^2)}$. Continuity of $z_{2\%}$ and its derivative with respect to ξ determine $c_2 = 0.25c_1^2/c_0$ and $p = 0.5c_1/c_0$. For each of the wave periods T_p; $T_{m-2,0}$; $T_{m-1,0}$; $T_{m0,1}$; and T_m, this formula was calibrated, while the optimal characteristic wave period was considered as the wave period with the smallest remaining scatter around the main trend. To quantify the scatter around the main trend, the root-mean-square of the relative deviation between the formula and the computations was used

$$\varepsilon = \sqrt{\frac{1}{i}\sum_{1}^{i}\left[\frac{(z_{2\%}/\gamma H_s)_{\text{formula}}}{(z_{2\%}/\gamma H_s)_{\text{calculated}}} - 1\right]^2} \tag{2}$$

Table 1 shows the values for ε that were obtained for each wave period and the optimal values of the coefficients c_0 and c_1. The values for c_0 and c_1 are not relevant, since these values do not indicate which of the wave periods is optimal. These values are influenced by the choice to use $\gamma = 0.7$ to account for the influence of roughness. Because of this choice and inaccuracies of the numerical model in general, the exact values for c_0 and c_1 need to be obtained from physical model tests.

Table 1 shows that the value for ε is the lowest for the wave period $T_{m-1,0}$. Therefore, it was concluded that the numerical model investigations indicate that, of those wave periods used in the analysis, the wave period $T_{m-1,0}$ is the optimal characteristic wave period for describing wave runup. This wave period was also found to be the optimal one for describing wave overtopping (van Gent 1999c). As already discussed by Battjes (1969), the best characteristic wave period for energy transport in random wave fields is also based on the spectral moments m_0 and m_{-1}.

TABLE 1. Influence of Using Different Characteristic Wave Periods (Computational Results)

Wave period	ε
T_p	0.147
$T_{m-2,0}$	0.064
$T_{m-1,0}$	0.057
$T_{m0,1}$	0.064
T_m	0.089

J. Waterway, Port, Coastal, Ocean Eng. 2001.127:254-262.

PHYSICAL MODEL TESTS

Physical model tests with three different foreshores and three different dike geometries were performed in a flume with active wave absorption (van Gent 1999a,b). These tests on wave runup and wave overtopping concern a systematic variation of the parameters (wave height, wave period, water depth, and spectral shapes), while a part of the tests was performed to reproduce six storms measured in prototype to gain insight into the differences between both types of measurements.

The first of the three foreshores corresponds to one for which prototype measurements were performed. The second foreshore is a straight 1:100 slope, and the third is a 1:250 slope. The dike geometries concern one that corresponds to the dike with a berm as in prototype, a straight 1:2.5 slope, and a straight 1:4 slope.

Storms Measured in Prototype

Prototype Measurements

Within the framework of the European MAST-OPTICREST project, prototype measurements on the Petten Sea defense in The Netherlands were performed by Rijkswaterstaat. This dike is of special interest, since the complex shallow foreshore affects the waves considerably before they reach the toe of the dike. The depth contours are rather parallel to the coast, while the mean angle of wave attack on the dike is nearly perpendicular. Therefore, it was considered feasible to model this prototype situation in a flume.

Fig. 3 shows the measured foreshore perpendicular to the Petten Sea defense. Between 7 and 3 km offshore, the depth gradually decreases from −20 m to −10 m (these levels are relative to the Dutch vertical reference level NAP), with an average slope of approximately 1:400. Then the foreshore shows an offshore bar with a crest at approximately −6 m, where wave breaking occurs during storms. Landward of the offshore bar, the depth increases again to −12 m at about 1 km from the dike. Fig. 4 shows a more detailed graph of the foreshore in the last kilometer, which was the part that was modeled in the physical model tests. A second bar with a crest at about −3.5 m is present at about 500 m seaward from the crest of the dike, where again wave breaking occurs during storms. The toe of the dike is again in shallow water, where for the third time a breaker zone is present.

The dike consists of a 1:4.5 lower slope, a berm of about 1:20, and a 1:3 upper slope. The crest elevation is at NAP + 12.9 m. The wave runup levels were measured at the upper slope by sensors, acting as a step gauge, within the smooth slope. Also in the physical model tests the measurements were performed on this upper slope (Fig. 5).

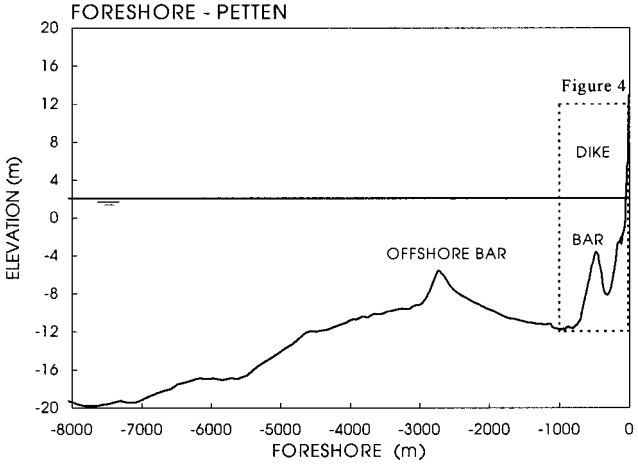

FIG. 3. Measured Foreshore Perpendicular to the Petten Sea-Defense

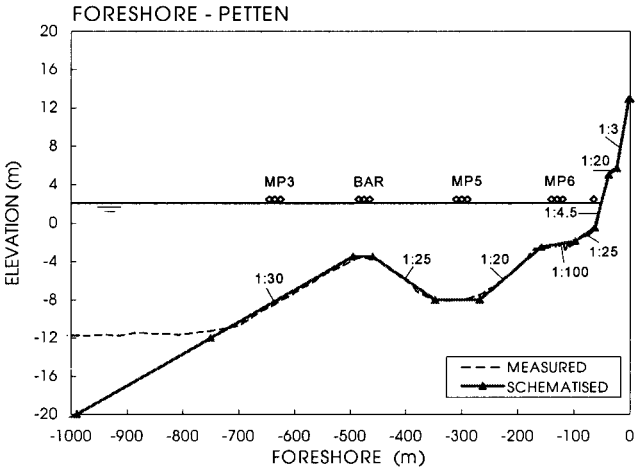

FIG. 4. Schematized Foreshore for Model Tests (Scale 1:40)

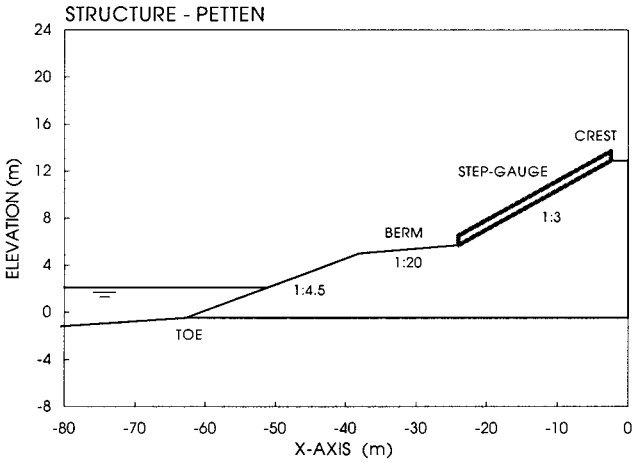

FIG. 5. Schematized Structure for Model Tests (Scale 1:40)

Wave conditions were measured at several positions between deep water and 65 m seaward of the crest of the dike; in Fig. 4 some of these locations in prototype are denoted (MP3, MP5, and MP6). Table 2 shows the storm conditions that were measured at MP3, MP5, and MP6, and the corresponding wave runup levels. The directional spreading according to a normal distribution was at deep water (NAP − 20 m, 8.3 km offshore) between 15° and 30° around the peak of the wave energy spectra. Since it is expected that further wave propagation to shallower water reduces the directional spreading, the magnitude of directional spreading at the toe of the dike is considered between small and normal.

Physical Model Tests for Comparison with Prototype Measurements

The last kilometer of the foreshore was modeled in a flume according to the schematization shown in Fig. 4 (scale of 1:40). For accurate wave generation, relatively deep water is desirable, to avoid the need to generate waves that are nearly breaking. Therefore, the water depth at the position of the wave board was increased with respect to the water depth at the corresponding position in the prototype situation; the front slope of the bar was extended to deeper water (Fig. 4). The wave board was equipped with active wave absorption (Kostense 1985) to reduce undesirable wave reflection at the wave board. The two bars on the foreshore in prototype both cause severe wave breaking under storm conditions. This causes the

J. Waterway, Port, Coastal, Ocean Eng. 2001.127:254-262.

TABLE 2. Measured Storms and Wave Runup Levels in Prototype (Data from Rijkswaterstaat-RIKZ)

Number	Date	MWL (NAP)	$H_{s\text{-}T}$ (MP3)	$T_{m-1,0}$ (MP3)	T_p (MP3)	$H_{s\text{-}T}$ (MP5)	$T_{m-1,0}$ (MP5)	T_p (MP5)	$H_{s\text{-}T}$ (MP6)	$T_{m-1,0}$ (MP6)	T_p (MP6)	$z_{2\%}$ (NAP)
1.01	1-1-95	2.10	4.24	8.9	11.1	2.61	8.7	11.1	2.94	9.2	12.5	8.3
1.02	1-1-95	2.01	4.24	8.6	11.1	2.65	8.7	11.1	2.81	9.1	12.5	7.6
1.03	2-1-95	2.18	3.84	10.2	16.7	2.61	9.9	7.1	2.99	10.8	20.0	8.7
1.04	2-1-95	1.64	4.24	10.4	16.7	2.39	10.1	16.7	2.64	10.8	12.5	6.9
1.05	2-1-95	1.60	3.08	9.8	14.3	2.37	9.6	14.3	2.60	9.8	14.3	6.4
1.06	10-1-95	2.00	3.70	8.8	10.0	2.66	9.0	11.1	2.78	9.4	9.1	7.7

Note: These wave conditions are based on the analysis of signals of surface elevations, including reflected waves, using the energy between frequencies 0.03 and 0.3 Hz (Δf = 0.01 Hz); there are approximately 500 waves per storm condition. NAP = Dutch vertical reference levels, wave heights $H_{s\text{-}T}$ are in meters, and wave periods $T_{m-1,0}$ and T_p are in seconds.

shapes of the energy density spectra at the toe of the structure to deviate considerably from the deep-water spectral shapes.

Since only the most landward bar could be modeled in the tests, the spectral shapes at the corresponding position of the wave board in the prototype situation were affected by wave breaking on the offshore bar. Therefore, for the tests where measured storms were modeled, the measured wave energy spectra were used, instead of standard spectral shapes such as Pierson-Moskowitz spectra or JONSWAP spectra. The waves, approximately 1,000 waves per wave condition, were generated such that at location MP3 the wave energy spectra were similar to those measured in prototype.

At several positions on the foreshore, wave conditions were measured in the model tests (Fig. 4 shows the position of the wave gauges)—at deep water, at the crest of the bar, at the toe of the structure, and at three positions where wave conditions have been measured in the prototype situation (MP3, MP5, and MP6). Fig. 6 shows an example of the evolution of wave heights over the foreshore, while Fig. 7 shows an example of the evolution of the wave energy spectra over the foreshore.

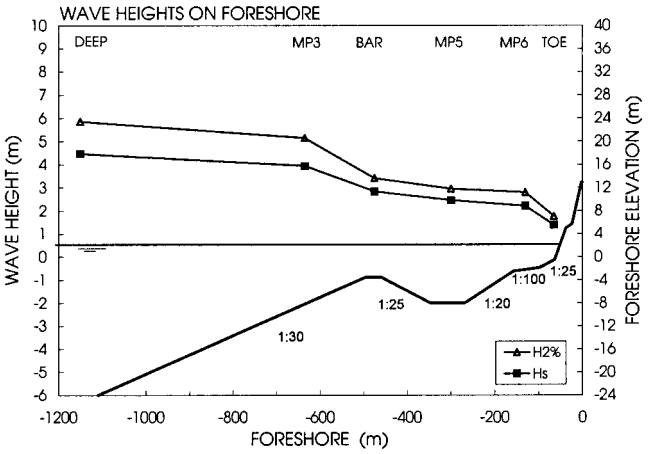

FIG. 6. Example of Evolution of Wave Heights over the Foreshore

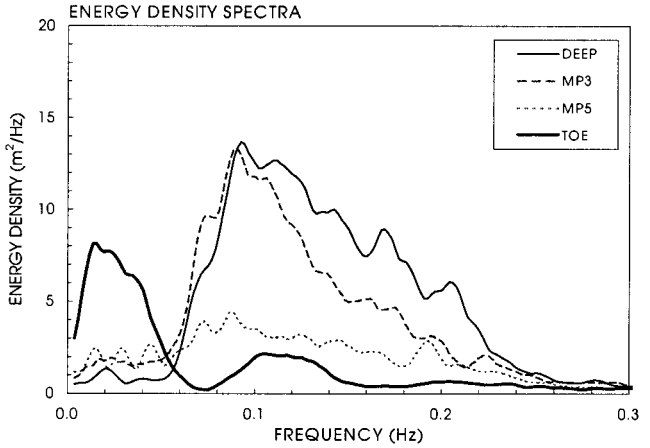

FIG. 7. Example of Evolution of Wave Energy Spectra over the Foreshore

In addition to the wave gauges, a step gauge to measure wave runup was installed. This step gauge consists of a beam with a large number of conductive probes. The probes were placed approximately 2.5 mm (model scale) above the slope such that water layers thinner than 2.5 mm were not recorded (i.e., 0.10 m on the prototype scale). The distance between the probes along the slope was 25 mm (model scale). The step gauge recorded for each probe the number of occasions that the probe came into contact with the water surface. Dividing this number by the number of incident waves yielded the probability of exceedance for each probe level, which provided, for instance, the wave runup levels that were exceeded by 2% of the incident waves, $z_{2\%}$. In addition to the step gauge, a wave gauge was positioned along the slope, which recorded wave runup levels at a level of approximately 5 mm (model scale) above the slope, in contrast to the step gauge, which recorded wave runup levels at a level of 2.5 mm above the slope. Similar to the prototype measurements, the wave runup levels were measured only on the section above the berm.

Comparison between Prototype Measurements and Physical Model Tests

Table 3 shows the comparison of the measured wave conditions at two locations (MP3 and MP6). The average difference between the measured significant wave heights (H_s = $H_{1/3}$) in prototype and in the model tests is at MP3 1.5%, at MP5 3.4%, and at MP6 8.8%. These differences can be caused by many factors, such as a slightly different foreshore during the actual storms than that used in the model tests, 3D effects, effects of wind, schematization effects, slightly different data acquisition and data analysis procedures, and scale effects. Nevertheless, the observed differences are considered acceptable to further investigate wave runup.

In prototype, thin water layers (between 0.02 m and 0.1 m) were also recorded as wave runup, while in the model tests, the step gauge could not record water layers thinner than 0.1 m (prototype scale). Therefore, comparison between the wave runup levels measured in prototype (indicated by P in Table 3), including thin water layers, and those measured with the step gauge in the model tests (indicated by M1 in Table 3), not including thin water layers, is not straightforward. However, linear extrapolations based on the measured wave runup levels with a minimum water layer of 0.1 m (step gauge) and the measured wave runup levels with a minimum water layer of 0.2 m (wave gauge along the slope) yield estimates of wave runup levels including thin water layers. These levels are indicated by M2 in Table 3. These M2 levels are used for comparison with the prototype measurements. A comparison is also made for the nondimensional wave runup level, where the

J. Waterway, Port, Coastal, Ocean Eng. 2001.127:254-262.

TABLE 3. Comparison beween Prototype Measurements and Physical Model Tests

	MWL (m) (MP3)		$H_{s\text{-}T}$ (m) (MP3)		$T_{m-1,0}$ (s) (MP3)		$H_{s\text{-}T}$ (m) (MP6)		$T_{m-1,0}$ (s) (MP6)		$z_{2\%}$ (m) (NAP)			$z_{2\%}/H_{s\text{-}T\text{-MP6}}$, Differences		
Test	P	M	P	M	P	M	P	M	P	M	P	M1	M2	P	M2	Percent
1.01	2.10	2.14	4.24	4.29	8.9	9.4	2.94	2.62	9.2	10.9	8.3	6.8	7.5	2.12	2.05	−3.3
1.02	2.01	2.01	4.24	4.13	8.6	9.5	2.81	2.56	9.1	11.0	7.6	6.9	7.4	1.99	2.09	5.1
1.03	2.18	2.21	3.84	3.83	10.2	10.7	2.99	2.69	10.8	12.1	8.7	7.5	8.4	2.17	2.30	6.0
1.04	1.64	1.62	4.24	4.38	10.4	11.5	2.64	2.53	10.8	12.4	6.9	6.9	7.1	1.99	2.15	7.9
1.05	1.60	1.59	3.08	3.08	9.8	10.3	2.60	2.30	9.8	11.1	6.4	5.8	5.8	1.86	1.81	3.0
1.06	2.00	2.02	3.70	3.76	8.8	9.5	2.78	2.58	9.4	11.4	7.7	6.8	7.3	2.04	2.04	0.0

Note: P = prototype, M = model tests, M1 = step-gauge result, and M2 = extrapolated to zero water layer.

wave runup level is the height above the *mean* water level [(MWL), relative to the NAP (m)] and the wave heights are the total significant wave heights ($H_s = H_{1/3}$) measured at MP6. Although wave runup levels are normally defined as the height above the *still* water level [(SWL), relative to the NAP (m)], the MWL has been used for this comparison because for the prototype circumstances the MWL is available, unlike the SWL. Except for this comparison with prototype data, in this paper the original definition is used (i.e., with respect to the SWL). The differences in percentage are listed in the last column of Table 3. The average of the differences (absolute values) is 4%, which is considered small. Nevertheless, differences can be caused by factors such as schematization and scale effects, related to, for instance, the roughness of the slope and the effects of wind on wave runup.

Errors introduced by schematization and scale effects related to roughness and wind are expected to be relatively important for thin water layers on the slope. These errors are to some extent avoided by not trying to measure these very thin layers, but by extrapolating from thicker layers that are expected to be less influenced by scale effects and wind. Although this (linear) extrapolation also introduces inaccuracies, this procedure provides at least an estimate of the runup levels, including thin water layers, and is considered better than neglecting the presence of these thin water layers in the comparison with the prototype measurements. For the purpose of studying the influence of several parameters on wave runup, this extrapolation is not necessary, and has therefore not been applied in the parameter analysis. Nevertheless, it should be kept in mind that neglecting thin water layers, as also done in the derivation of design formulas based on physical model tests, can provide nonconservative estimates. The results shown in Table 3 indicate that the estimates with formulas based on tests neglecting the thin water layers may be on the order of 10% too low compared to reality. To evaluate this estimate, further research on, for instance, the influence of wind on wave runup, especially its effects on thin water layers, is needed.

Systematic Variation of Parameters

Description of Physical Model Tests

A systematic variation of parameters was performed to study which characteristic wave height and which characteristic wave period account for the effects of wave height distributions and wave energy spectra, respectively, on wave runup and wave overtopping. For this purpose, the following combinations of foreshore and slope of the dike were used:

- Foreshore 1:100 with a 1:4 dike (Fig. 8)
- Foreshore 1:100 with a 1:2.5 dike
- Foreshore 1:250 with a 1:2.5 dike

The test program consisted of tests with single and double-peaked wave energy spectra, represented by wave trains of approximately 1,000 waves. Tests with four water levels were performed such that wave conditions at the toe of the structure varied, denoted by ''deep'' (although the conditions do not necessarily correspond to deep-water conditions at the toe), ''intermediate,'' ''shallow,'' and ''very shallow'' (Fig. 8). A wide range of values of the surf-similarity parameter (at the toe of the structure) was obtained by variation of the following parameters (at the wave board, denoted by deep):

1. The water depth
   - For single-peaked wave energy spectra between $H_{m0\text{-DEEP}}/d_{\text{TOE}} = 0.4$ and 3
   - For double-peaked wave energy spectra between $H_{m0\text{-DEEP}}/d_{\text{TOE}} = 0.4$ and 1.5
2. The wave steepness
   - For single-peaked wave energy spectra between $s_{-1} = 0.018$ and 0.044
   - For double-peaked wave energy spectra between $s_{-1} = 0.020$ and 0.051
3. The spectral shape
   - For single-peaked wave energy spectra, JONSWAP spectra were used.
   - For double-peaked wave energy spectra, use was made of a superposition of two JONSWAP spectra. The distance between the two individual peaks was varied ($T_{p2}/T_{p1} = 0.4-1.0$), as was the ratio between the amount of energy in each individual JONSWAP spectrum ($m_{0(2)}/m_{0(1)} = 0.5-2.0$).
   - Fig. 9 shows examples of wave energy spectra used in the tests.

The tests with single-peaked wave energy spectra were primarily performed to study the effects of wave height distributions on wave runup and wave overtopping. As reference tests, conditions were tested for which the wave height distribution at the toe was expected to be close to the Rayleigh distribution, as is the case in deep water (denoted by deep in

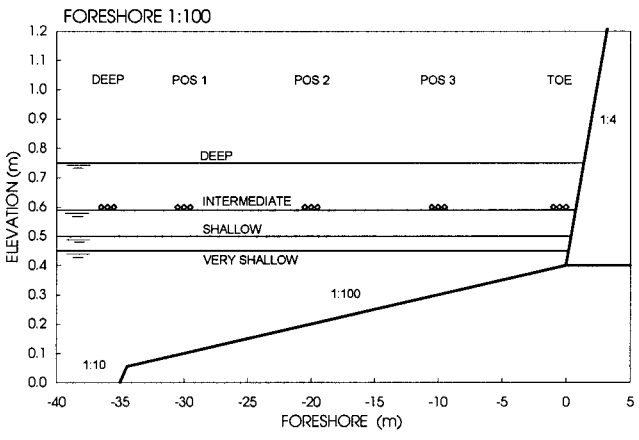

FIG. 8. Foreshore 1:100 and a 1:4 Slope

J. Waterway, Port, Coastal, Ocean Eng. 2001.127:254-262.

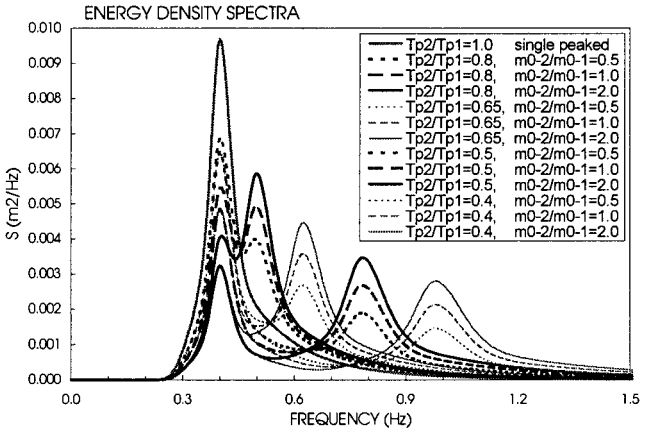

FIG. 9. Examples of Double-Peaked Wave Energy Spectra in Model Tests

Fig. 8). Tests with lower water levels were performed to study wave runup and wave overtopping in situations of non-Rayleigh distributed wave height distributions. The generated wave energy spectra were single peaked, which did not necessarily mean that at the toe of the structure the wave energy spectra were single peaked; the foreshore may cause the single-peaked wave energy spectra to transform into double-peaked wave energy spectra. Moreover, due to the presence of the foreshore, the systematic variation of parameters of the generated spectra did not necessarily lead to the same systematic variation of parameters at the toe of the structure. For instance, the wave energy in the peak with the higher frequency may be more susceptible to wave breaking than the wave energy in the peak with a lower frequency, such that the ratio between the energy in both peaks changes. Nevertheless, in most tests, variations in the wave energy spectra at deep water resulted in variations in the wave energy spectra at the toe, such that the wave energy spectra at the toe still sufficiently varied in shape to allow for the study of the effects of different wave energy spectra.

Common analysis procedures for wave runup and wave overtopping require the wave height of the incident waves at the toe of the dike as input. The method used here to extract both the incident waves and the reflected waves from measured wave height recordings [based on Mansard and Funke (1981)] requires signals from (three) wave gauges relatively close to each other, consequently leading to a lower accuracy for the energy density in the lower frequencies. Since the toe of the structure is for a series of tests in relatively shallow water with breaking waves, while these techniques assume nonbreaking waves, this method is not always applied with high accuracy. Nevertheless, this technique was used to obtain the incident waves at the position of the toe during tests without the structure in position, with a horizontal part of 5 m between ''toe'' and a dissipating beach profile. This was done because the dissipating beach does still cause some reflection of wave energy. The procedure to repeat the tests without the structure in position also introduces undesirable effects, since in reality waves reflected by the dike interact with incident waves; these processes are not modeled correctly in tests without the dike in position. This is especially the case for these conditions where wave breaking in shallow water takes place and surfbeat phenomena (the propagation of wave groups and their associated long wave motion), for which wave reflection is important, play a role.

Analysis of Test Results

The data set was analyzed to study which characteristic wave height and which characteristic wave period can best be used in the surf-similarity parameter to describe wave runup and wave overtopping. Three characteristic wave heights were used in the analysis—the significant wave height H_s, i.e., $H_{1/3}$; the wave height exceeded by 2% of the waves, $H_{2\%}$ (time-domain analysis); and the wave height H_{m0} (spectral analysis). These wave heights were based on the incident waves at the toe and on the entire wave energy spectra, including energy in the low frequency waves. The conclusion was that each of the three characteristic parameters studied is considered to be a suitable characteristic wave height to describe wave runup and wave overtopping. Here, the significant wave height H_s is used for analysis of the optimal characteristic wave period, although the conclusions do not differ if one uses one of the other two wave heights.

For wave conditions with very shallow water, there is a significant transfer of wave energy to lower frequencies, which for some situations results in a peak wave period that is almost 10 times longer than the peak wave period at deep water. This is caused by surfbeat phenomena. This also results in rather extreme values for the surf-similarity parameter, especially if the peak wave period T_p is used, but also if the wave period $T_{m-1,0}$ is used. The mean wave period T_m is less sensitive to this transfer of energy to long waves. Fig. 10 shows the measured wave runup levels as a function of the surf-similarity parameter using the wave period $T_{m-1,0}$ (based on the incident waves at the toe and on the entire wave energy spectra, including energy in the low frequency waves).

Similar to the analysis of the computational results, again (1) is used to describe the main trend through the data. For each of the wave periods T_p; $T_{m-2,0}$; $T_{m1,0}$; $T_{m0.1}$; and T_m, this formula was calibrated, while the optimal characteristic wave period was considered as the wave period with the smallest remaining scatter around the main trend. To quantify the scatter around the main trend, again the root-mean-square of the relative deviation between the formula and the computations was used [(2) with $\gamma = 1$]. Table 4 shows the optimal values of the coefficients c_0, c_1, and ε, where the significant wave height of the incident waves at the toe of the structure, obtained from time-domain analysis ($H_s = H_{1/3}$), is used as the characteristic wave height.

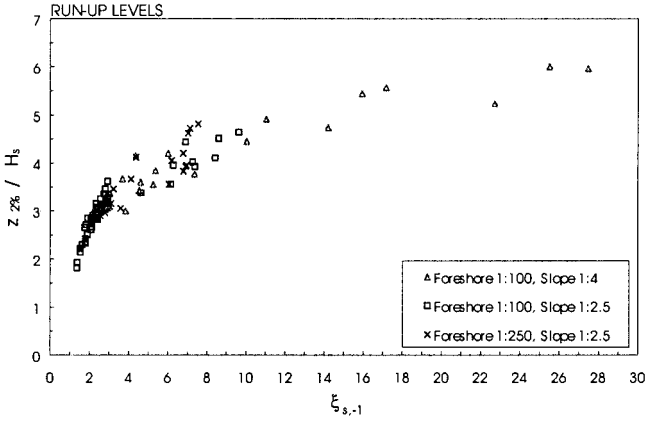

FIG. 10. Measured 2% Wave Runup Levels As Function of the Surf-Similarity Parameter Based on the Wave Period $T_{m-1,0}$

TABLE 4. Influence of Using Different Characteristic Wave Periods (Physical Model Tests)

Wave period	c_0	c_1	ε
T_p	1.35	4.3	0.104
$T_{m-2,0}$	1.2	4.4	0.105
$T_{m-1,0}$	1.35	4.7	0.084
$T_{m0,1}$	1.8	5.1	0.112
T_m	1.95	5.2	0.143

J. Waterway, Port, Coastal, Ocean Eng. 2001.127:254-262.

Thus, similar to the computational results, again the wave period $T_{m-1,0}$ performs better than the other wave periods. The same conclusion was found after the analysis of the measured wave overtopping discharges. Of those wave periods used in the analysis, the most suitable characteristic wave period to describe wave runup and wave overtopping is $T_{m-1,0}$.

PREDICTION METHODS

The physical model tests described in the previous section, together with data by Smith (1999) and an additional systematic variation of parameters on the structure with a foreshore with the bar (storms measured in prototype section), are used for comparison with two formulas to predict wave runup levels. Both are extensions of formulas by Hunt (1959) and Battjes (1974), where wave runup was expressed as a function of the surf-similarity parameter, combining the influences of wave height, wave period, and slope angle. The first formula applied here was not derived for situations with shallow foreshores, although it is frequently applied for such conditions because of the lack of other prediction methods. The second formula aims at a relatively generic method for predicting wave runup levels, irrespective of whether a situation with deep water at the toe or a situation with shallow water is regarded.

The first formula is the one by De Waal and van der Meer (1993), where reduction factors are incorporated for the influences of roughness, foreshores, angular wave attack, and berms

$$z_{2\%}/(\gamma H_s) = c_0 \xi_{op} \quad \text{for } \xi_{op} \leq p \tag{3a}$$

$$z_{2\%}/(\gamma H_s) = c_1 \quad \text{for } \xi_{op} \geq p \tag{3b}$$

where γ = reduction factor that takes the effects of roughness (γ_f) and angular wave attack (γ_β) into account; $\gamma = \gamma_f \gamma_\beta$. Based on a reanalysis of data on wave overtopping, van der Meer (1997) proposed not to use the originally proposed reduction factor for foreshores. The coefficients c_0, c_1, and p in (3) were set at 1.5, 3, and 2 based on physical model tests. For design purposes, it was advised to use somewhat safer values, 1.6, 3.2, and 2, respectively. The wave conditions used in (3) are the significant wave height of the incident waves at the toe of the structure ($H_{1/3}$) and the peak wave period T_p at deep water. Eq. (3) has often been applied in combination with the geometric methods discussed in the numerical modeling section to account for the effects of double-peaked wave energy spectra. Because the peak wave period, or an equivalent peak wave period obtained from such geometric methods, is based on wave energy spectra at deep water, one is neglecting the changes in the wave energy spectra between deep water and the toe of the structure. This is, for instance, the case for situations where single-peaked wave energy spectra at deep water transform into double or multipeaked wave energy spectra. Here, no geometric method to account for the effects of double-peaked wave energy spectra has been used in combination with (3). Therefore, the comparison of (3) with data shows the effects of using a deep-water wave period in the predictions, without the effects of remedies to handle nonstandard wave energy spectra at deep water.

One data set (storms measured in prototype section) concerns a dike with a berm. Besides a characteristic wave height and characteristic wave period, such geometry also requires a characteristic slope to be used in the surf-similarity parameter. In van Gent (2000), three methods to take into account the effects of berms are studied based on data sets from numerical modeling and physical model tests. Similar to the numerical data set described in the numerical modeling section, a data set was created for a wide range of berm configurations (94 in total), with berms with a width between $2 \leq B/H_s \leq 6$ that start at levels, with respect to the still water level, between $-1 \leq h_{\text{BERM}}/H_s \leq 1$. The computations and physical model tests indicated that the simple method shown in Fig. 11 is appropriate, and that for this method no additional reduction factor for berms is required. The characteristic slope was defined as $\tan\varphi = 2c_{\text{BERM}}H_s/L$, where c_{BERM} was set at 2, which has also been used here in the analysis of the tests.

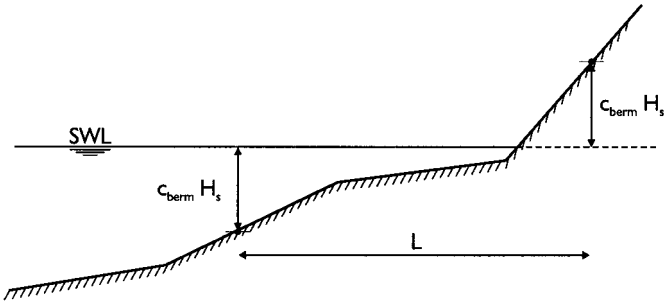

FIG. 11. Method to Obtain a Characteristic Slope (van Gent 2000)

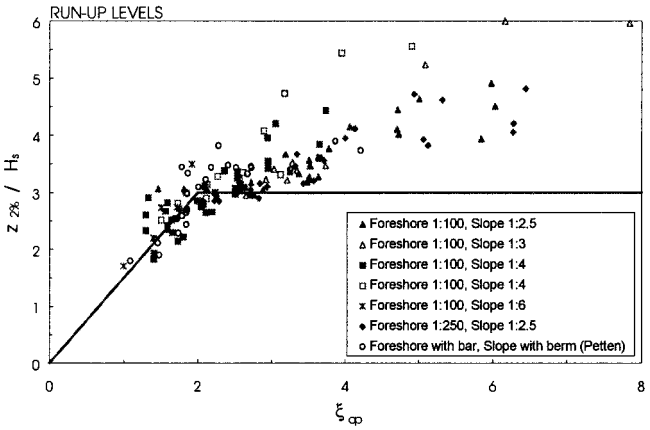

FIG. 12. Comparison between Measured and Calculated Wave Runup Levels, Using (3)

Fig. 12 shows the comparison between (3) and the measurements. In this formula, the deep-water peak wave period is used, which is expected to cause the large scatter without a clear trend; the foreshore considerably affects the wave conditions, including a change in the peak wave period between the deep water and the toe of the structure. This figure clearly indicates that (3) in combination with the deep-water peak wave period is not appropriate for shallow foreshores and may lead to significant underestimates of wave runup. If one uses the peak wave period at the toe of the structure, the predictions improve for the low values of the surf-similarity parameter, but for the conditions with relatively shallow foreshores, often leading to higher values of the surf-similarity parameter, the comparison does not significantly improve.

To account for arbitrary spectral shapes and to derive a formula with a smooth transition at a certain value of the surf-similarity parameter, a prediction formula was proposed in van Gent (1999c). In this formula, as already given in (1), the wave period $T_{m-1,0}$ is used in the surf-similarity parameter

$$z_{2\%}/(\gamma H_s) = c_0 \xi_{s,-1} \quad \text{for } \xi_{s,-1} \leq p \tag{4a}$$

$$z_{2\%}/(\gamma H_s) = c_1 - c_2/\xi_{s,-1} \quad \text{for } \xi_{s,-1} \geq p \tag{4b}$$

where H_s = significant wave height of the incident waves at the toe of the structure ($H_s = H_{1/3}$). The reduction factor γ ($\gamma = \gamma_f \gamma_\beta$) takes the effects of angular wave attack (γ_β) and roughness (γ_f) into account. The surf-similarity parameter is defined as $\xi_{s,-1} = \tan\varphi/\sqrt{(2\pi/g \cdot H_s/T_{m-1,0}^2)}$. The continuity of $z_{2\%}$ and its derivative with respect to $\xi_{s,-1}$ determine $c_2 = 0.25c_1^2/c_0$ and $p = 0.5c_1/c_0$. Eq. (4) was calibrated based on the

J. Waterway, Port, Coastal, Ocean Eng. 2001.127:254-262.

described physical model tests (systematic variation of parameters section); $c_0 = 1.35$ and $c_1 = 4.7$ (with a standard deviation of 0.37). Fig. 13 shows all data with a surf-similarity parameter smaller than 12 (Fig. 10 shows a few data points with a surf-similarity parameter larger than 12). This figure shows that (4) leads to a relatively low amount of scatter and an adequate description of the trend. It can be concluded that improving the method to predict wave runup by using the wave period $T_{m-1,0}$ at the toe of the structure instead of the peak wave period at deep water, and calibrating (4) improve the predictions of wave runup. Most data concerned situations in the range of $1 < \xi_{s,-1} < 10$, in which $2.5 \leq \tan \varphi \leq 6$. To what extent the application of (4) outside these ranges is appropriate still needs to be investigated.

The analysis so far was based on the entire wave energy spectra (except for the comparison with the prototype measurements), which means that both the energy in the long waves and the energy in the short waves contribute to the values of the wave parameters. Alternatively, the analysis can be based on the wave parameters obtained from energy in the short waves only. If the prediction method that provides the wave conditions at the toe of the structure provides wave conditions based on short waves only, one might prefer to use (4), in which the coefficients are calibrated based on the short waves only. Table 5 shows the results of these calibrations, where either the spectral ''significant wave height'' H_{m0} or the significant wave height from the time-domain analysis ($H_s = H_{1/3}$) is used as the characteristic wave height. One set of coefficients can be used if the wave parameters are based on the energy in the entire wave energy spectrum, including both long and short waves, and one set of coefficients can be used if the wave parameters are based on the energy in the short waves only. The corresponding standard deviations σ are given to facilitate the use in probabilistic procedures.

The values given in Table 5 neglect water layers thinner than approximately 0.1 m. If these thin water layers are to be accounted for, the values for c_0 and c_1 are expected to be approximately 10% higher.

To use (4) in practical situations, with the coefficients shown in Table 5, one may need to predict the wave parameters at the toe of the structure with a numerical model. In van Gent and Doorn (2001), it was shown that the Boussinesq-type model by Borsboom et al. (2001) can rather accurately predict these wave conditions for situations with severe wave breaking on shallow foreshores.

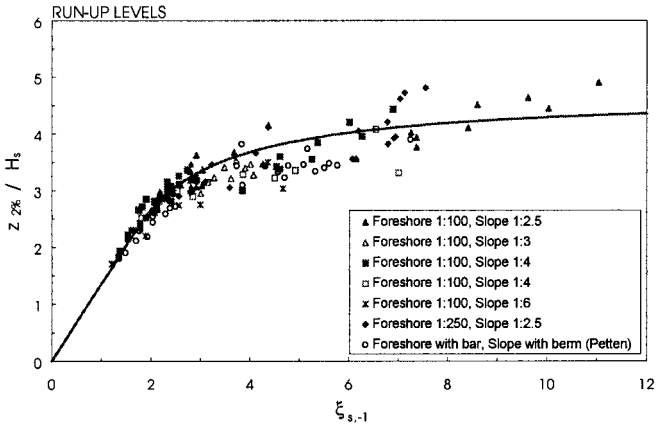

FIG. 13. Comparison between Measured and Calculated Wave Runup Levels, Using the Present Calibration of (4)

TABLE 5. Coefficients in (4) for Wave Runup Predictions; $c_2 = 0.25c_1^2/c_0$ and $p = 0.5c_1/c_0$

Wave energy spectra	Wave height	Wave period	c_0	c_1	σ
Total: long and short waves	H_{m0}	$T_{m-1,0}$	1.45	3.8	0.24
Total: long and short waves	H_s	$T_{m-1,0}$	1.35	4.7	0.37
Short waves only	H_{m0}	$T_{m-1,0}$	1.45	5.0	0.51
Short waves only	H_s	$T_{m-1,0}$	1.55	5.4	0.63

CONCLUSIONS

These investigations, which made use of a combination of prototype measurements, physical modeling, and numerical modeling, lead to the following conclusions:

- Comparisons between storms measured in prototype and storms modeled in the physical model tests show good agreement. The nondimensional wave runup levels differ by only 4% on average; considering the observed differences between the prototype measurements and the physical model tests, it can be concluded that the schematization and scale effects in the physical model tests are small.
- Numerical model computations support the use of the wave period $T_{m-1,0}$ at the toe of coastal structures to account for the effects of wave energy spectra on wave runup. This is in conformance with the characteristic wave period by Battjes (1969) for wave energy transport.
- Physical model tests also support the use of the wave period $T_{m-1,0}$ at the toe of coastal structures to account for the effects of wave energy spectra on wave runup. The physical model tests also showed that for the characteristic wave height, each of the three wave heights H_{m0}, H_s, and $H_{2\%}$ is suitable to account for the influence of wave height distributions on wave runup. In van Gent (1999a), it was shown that these conclusions are also valid for wave overtopping.
- Using the peak wave period in predictions on wave runup may lead to large inaccuracies for situations with shallow foreshores.
- A smooth and simple formula for wave runup on coastal structures is proposed, with a gradual curve toward an upper limit of the nondimensional wave runup [(4)]. This formula is rather generic because it can be used for situations with relatively deep water at the toe of coastal structures and for situations with shallow foreshores. The influence of wave energy spectra on wave runup is accounted for by using the spectral wave period $T_{m-1,0}$ of the incident waves at the toe of coastal structures.

ACKNOWLEDGMENTS

The research presented here is partly performed within the European research project MAST-OPTICREST (contract MAS3-CT97-0116) and partly in cooperation with Rijkswaterstaat-DWW. The data on the prototype measurements at the Petten Sea defense were kindly provided by Rijkswaterstaat-RIKZ. Prof. Dr. J. A. Battjes of the Delft University of Technology is gratefully acknowledged for his valuable contributions and reviews of the reports on which this paper is based.

REFERENCES

Battjes, J. A. (1969). ''Discussion of paper by J. N. Svašek: 'Statistical evaluation of wave conditions in a deltaic area.' '' *Proc., Symp. on Res. on Wave Action*, Vol. 1, Paper 1, Delft Hydraulics, Delft, The Netherlands.

Battjes, J. A. (1974). ''Computation of set-up, longshore currents, runup and overtopping due to wind-generated waves.'' PhD thesis, Department of Civil Engineering, Delft University of Technology, Delft, The Netherlands.

Borsboom, M., Doorn, N., Groeneweg, J., and van Gent, M. (2001). ''A Boussinesq-type wave model that conserves both mass and momentum.'' *Proc., ICCE 2000*, Vol. 1, ASCE, Reston, Va., 148–161.

Bouws, E., Günther, H., Rosenthal, W., and Vincent, C. L. (1985). ''Similarity of the wind wave spectrum in finite depth water. 1. Spectral form.'' *J. Geophys. Res.*, 90(C1), 975–986.

J. Waterway, Port, Coastal, Ocean Eng. 2001.127:254-262.

Cornett, A., and Mansard, E. (1995). ''Wave stresses on rubble mound armour.'' *Proc., ICCE'94*, Vol. 1, ASCE, New York, 986–1000.
De Waal, J. P., and van der Meer, J. W. (1993). ''Wave run-up and overtopping on coastal structures.'' *Proc., ICCE'92*, Vol. 2, ASCE, New York, 1758–1771.
Hibberd, S., and Peregrine, D. H. (1979). ''Surf and run-up on a beach: A uniform bore.'' *J. Fluid Mech.*, Cambridge, England, 95(Part 2), 323–345.
Holterman, S. (1998). ''Golfoploop op dijken met ondiepe voorlanden [Wave run-up at dikes with shallow foreshores].'' MSc thesis, Delft University of Technology, Delft, The Netherlands (in Dutch).
Hunt, I. A. (1959). ''Design of seawalls and breakwaters.'' *Trans. ASCE*, New York, 85(3), 123–152.
Kobayashi, N., Otta, A. K., and Roy, I. (1987). ''Wave reflection and run-up on rough slopes.'' *J. Wtrwy., Port, Coast., and Oc. Engrg.*, ASCE, 113(3), 282–298.
Kostense, J. K. (1985). ''Measurements of surf beat and set-down beneath wave group.'' *Proc., ICCE'84*, ASCE, New York, 724–740.
Mansard, E. F. P., and Funke, E. (1981). ''The measurement of incident and reflected spectra using a least-squares method.'' *Proc., ICCE'80*, ASCE, New York, 154–172.
Seijffert, J. J. W. (1991). ''Golfoploop bij tweetoppig spectrum [Wave run-up for double peaked spectrum].'' Note, Rijkswaterstaat-DWW, Delft, The Netherlands (in Dutch).
Smith, G. M. (1999). ''Oploop—en overslagmetingen op een ondiep voorland [Wave run-up and wave overtopping measurements for a shallow foreshore].''*Rep. H3271/H3471*, Delft Hydraulics, Delft, The Netherlands (in Dutch).
van der Meer, J. W. (1997). ''Golfoploop en golfoverslag bij dijken [Wave run-up and wave overtopping at dikes].'' *Rep. H2458/H3051*, Delft Hydraulics, Delft, The Netherlands (in Dutch).
van Gent, M. R. A. (1994). ''The modelling of wave action on and in coastal structures.'' *Coast. Engrg.*, 22(3-4), 311–339.
van Gent, M. R. A. (1995). ''Wave interaction with permeable coastal structures.'' PhD thesis, Delft University of Technology, Delft, The Netherlands.
van Gent, M. R. A. (1999a). ''Physical model investigations on coastal structures with shallow foreshores: 2D model tests on the Petten Sea-defence.'' *MAST-OPTICREST Rep. and Delft Hydr. Rep. H3129*, Delft Hydraulics, Delft, The Netherlands.
van Gent, M. R. A. (1999b). ''Physical model investigations on coastal structures with shallow foreshores: 2D model tests with single and double-peaked wave energy spectra.'' *Rep. H3608*, Delft Hydraulics, Delft, The Netherlands.
van Gent, M. R. A. (1999c). ''Wave run-up and wave overtopping for double-peaked wave energy spectra.'' *Rep. H3351*, Delft Hydraulics, Delft, The Netherlands.
van Gent, M. R. A. (2000). ''Wave run-up on dikes with berms.'' *Rep. H3205*, Delft Hydraulics, Delft, The Netherlands.
van Gent, M. R. A., and Doorn, N. (2001). ''Numerical model simulations on wave propagation and wave run-up on dikes with shallow foreshores.'' *Proc., Coast. Dyn. 2001*, ASCE, Reston, Va., 769–778.
Van Oorschot, J. H., and d'Angremond, K. (1969). ''Chapter 57: The effect of wave energy spectra on wave run-up.'' *Proc., ICCE'68*, ASCE, New York, 886–900.

NOTATION

The following symbols are used in this paper:

B = berm width (m);
c_{BERM} = coefficient in method to obtain characteristic slope (-);
D_{n50} = stone diameter, exceeded by 50% of material (m);
d_{TOE} = water depth at toe of structure (m);
f = friction coefficient in numerical computations (-);
g = gravitational acceleration (m/s^2);
H_{m0} = spectral significant wave height, $H_{m0} = 4\sqrt{m_0}$ (m);
H_s = significant wave height; mean of highest one-third of waves; $H_{1/3}$ (m);
$H_{s\text{-}T}$ = total significant wave height, including reflected waves (m);
$H_{1/3}$ = significant wave height; mean of highest one-third of waves (m);
h_{BERM} = height of start of berm, relative to still water level (m);
L = length to obtain reduction factor for berms (m);
m_n = nth moment of frequency spectrum;
m_0 = variance of water surface elevation; i.e., total wave energy (m^2);
$m_{0(1)}$ = m_0 of first peak in double peaked spectrum (m^2);
$m_{0(2)}$ = m_0 of second peak in double peaked spectrum (m^2);
S = energy density (m^2/Hz);
s_{op} = wave steepness based on H_s at toe and T_p in deep water (-);
s_{-1} = wave steepness based on spectral wave period, $s_{-1} = 2\pi/g \cdot H_s/T^2_{m-1,0}$ (-);
T_m = mean wave period from time domain analysis (s);
$T_{m0,1}$ = wave period based on zeroth and first spectral moment (s);
$T_{m-1,0}$ = wave period based on zeroth and first negative spectral moment (s);
$T_{m-2,0}$ = wave period based on zeroth and second negative spectral moment (s);
T_p = peak wave period, defined as wave period in arbitrary wave energy spectrum where spectral density has global maximum (s);
T_{p1} = wave period of first peak in double peaked spectrum (s);
T_{p2} = wave period of second peak in double peaked spectrum (s);
$z_{2\%}$ = wave runup level exceeded by 2% of incident waves, relative to still water level unless denoted otherwise (m);
β = angle of wave attack (°);
γ = reduction factor for wave runup (-);
γ_β = reduction factor for wave runup, due to angular wave attack (-);
γ_f = reduction factor for wave runup, due to roughness (-);
ε = root-mean-square error (-);
ξ_m = surf-similarity parameter at toe of structure, $\xi_m = \tan\varphi/\sqrt{(2\pi/g \cdot H_s/T^2_m)}$ (-);
ξ_{op} = surf-similarity parameter based on wave height at toe and peak wave period at deep water, $\xi_{op} = \tan\varphi/\sqrt{(2\pi/g \cdot H_s/T^2_{p\text{-deep}})}$ (-);
ξ_p = surf-similarity parameter at toe of structure, $\xi_p = \tan\varphi/\sqrt{(2\pi/g \cdot H_s/T^2_p)}$ (-);
$\xi_{s,-1}$ = surf-similarity parameter at toe of structure, $\xi_{s,-1} = \tan\varphi/\sqrt{(2\pi/g \cdot H_s/T^2_{m-1,0})}$ (-);
σ = standard deviation (-); and
φ = slope of structure (°).